A NEW NONRIGID REGISTRATION FRAMEWORK FOR IMPROVED VISUALIZATION OF TRANSMURAL PERFUSION GRADIENTS ON CARDIAC FIRST-PASS PERFUSION MRI

Fahmi Khalifa[1], *Garth M. Beache*[2], *Georgy Gimel'farb*[3], *and Ayman El-Baz*[1*]

[1]BioImaging Laboratory, Bioengineering Department,University of Louisville, Louisville, KY, USA.
[2]Radiology Department, School of Medicine, University of Louisville, Louisville, KY, USA.
[3]Department of Computer Science, University of Auckland, Auckland, New Zealand.

ABSTRACT

A new framework for accurate registration of the segmented left ventricle (LV) on cardiac first-pass magnetic resonance imaging (FP-MRI) to precisely analyze the myocardial transit of contrast agent, especially in the ischemically damaged heart, is proposed. Due to the continuous physiological motion of the heart that causes the LV wall to change shape significantly, within the same scan, at the same cross section, we propose a new registration methodology that involves three steps: (i) global target-to-reference frame-to-frame alignment based on maximizing normalized mutual information (NMI); (ii) local alignment based on using a B–splines transformation model that maximizes a new similarity function that accounts for the 1st– and 2nd–order NMI between the globally aligned frames followed by (iii) a refinement step which is based on deforming each pixel of the target wall over evolving closed equi–spaced contours (iso–contours) to closely match the reference wall. Respective iso–contours in both reference and target frames are matched based on solving the Laplace equation. We have tested our framework on 20 FP-MRI datasets that have been collected from patients with is-chemic damage resulting from heart attacks and who are undergoing experimental therapy, and have documented an improvement in the visualization and display of perfusion–related indexes.

Index Terms— Perfusion MRI, nonrigid registration, functional mapping, ischemic heart disease.

1. INTRODUCTION

Cardiac and respiratory motion causes the heart to move within and through the image plane, as the heart progresses through its periodic cycle. Also, the heart undergoes large shape changes as it contracts. These rigid and nonrigid changes limit quantification of perfusion parameters on time series data. Importantly, unlike late gadolin-ium assessments which essentially characterize a steady physiologic state, first-pass perfusion characterizes a dynamic state and thus has challenges related to limitations of temporal sampling, of the gated cardiac images. To improve spatial correspondence of regions–of–interest, the first-pass temporal data must be registered to compen-sate for artifacts from patient motion, breathing, and heart contrac-tion. However, the registration is subject to multiple challenges stemming from highly nonrigid deformations, low signal to noise ratio, and large variation of the contrast enhanced image intensities.

A number of registration approaches have been introduced to correct the motion of the heart on perfusion images. In particular, Breeuwer et al. [1] proposed a translation / rotation-based rigid reg-istration approach, using normalized cross-correlation (NCC) as a

similarity measure. A similar approach was proposed by Wong et al. [2] using normalized mutual information (NMI) as a similarity metric. Bidaut and Vallee [3] introduced a multiresolution registra-tion approach employing cardiac masks to restrict the registration to the area of the nearly rigid motion of the heart. Their approach is based on minimizing the mean squared differences (MSD) between perfusion sequence images and the reference image. Gallippi et al. [4] corrected the cardiac motion using a statistics-based registra-tion approach. All of the images are registered to the central image of the perfusion sequence using intensity variations and edge directions as similarity measures. Stegmann et al. [5] proposed the use of ac-tive appearance models (AAMs) to segment the LV and to compen-sate for motion in the perfusion images. Adluru et al. [6] proposed an iterative model-based registration approach whereby the distance between the actual and ideal perfusion curve are used as a criterion for registration. Milles et al. [7] proposed a two-pass, coarse-to-fine, registration approach using independent component analysis (ICA) to deal with local intensity change of the perfusion images. In their framework, each image frame is registered to a time-varying refer-ence image that is constructed from three identified images of the left and the right ventricle intensity curves using ICA. The registration is achieved based on minimizing the sum of squared differences.

Recently, Wollny et al. [8] proposed a multiresolution nonrigid registration approach based on the quasi-periodicity of respiratory motion. Their registration framework uses a semi–local B-splines parametric transformation to optimize the normalized gradient field (NGF) similarity metric. To compensate for cardiac translation and deformation, Tarroni et al. [9] proposed a nonrigid registration algo-rithm using a 2D multi-scale extension of NCC. In their approach, each image frame is registered to both a template frame and five other additional frames created by resizing the reference frame. The transformation parameters are determined according to the template with peak cross-correlation value, and then contour adaptation was achieved using an edge-based level set method.

In summary, the above-mentioned approaches show the follow-ing limitations: (i) most of the methods heavily depend on image intensity for thresholding or extracting image features; (ii) most of them depend on using rigid registration only and do not account for the nonrigid deformations of the heart; (iii) parametric shape based approaches depend on the existence of good texture features in per-fusion images and may perform poorly on some frames due to noise and the lack of well-defined features. To overcome these limitations, we propose a novel framework for accurate nonrigid registration of FP-MRI that has the ability to handle large deformations of the heart to precisely analyze the the myocardial transit of contrast agent. In this paper, we will focus on accurate registration of the FP-MRI data. The segmentation of the LV wall borders is fully described in [10].

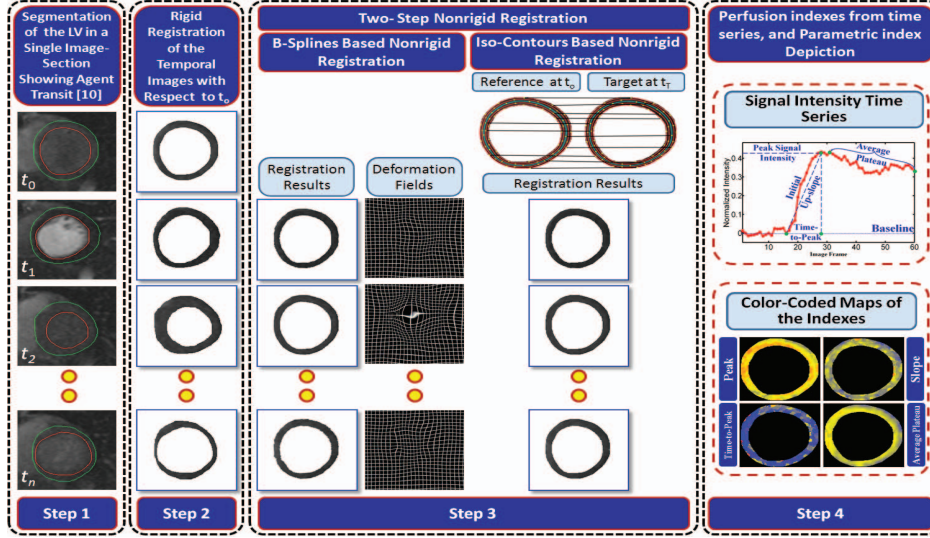*Corresponding author:- Tel:(502)-852-5092, Fax:(502)-852-6806, E-mail: aselba01@louisville.edu

Fig. 1. The proposed framework for analyzing first-pass perfusion MRI.

(a)

(b)

Fig. 2. Marginal (a) and joint (b) 2nd–order MGRF model for the reference and target images.

2. MATERIAL AND METHODS

We propose a new registration framework for the improved visualization of transmural perfusion gradients on cardiac FP-MRI. The proposed framework begins with segmented LV walls from the FP-MRI data and consists of three main steps (see Fig. 1). Each step will be discussed in detail in the following sections.

2.1. Rigid Registration

The registration of cardiac FP-MRI remains the most challenging task due to the high deformations related to heart contraction and respiratory motion. In order to capture the global motion of the heart, the segmented myocardial walls are co-aligned by a rigid, 2D affine transformation based on maximizing the NMI (the similarity measure) [11]. The result of the NMI-based rigid alignment for one image frame is demonstrated in Fig. 6(c).

2.2. Nonrigid Registration

Because of the large deformations in the LV shape due to heart contraction and respiratory motion during MRI acquisition, elastic, spatially variant, local warping models are needed for its correction. In this paper, we propose a two-step nonrigid registration approach to handle these deformations, the details of which are outlined below.

2.2.1. B–splines based nonrigid registration

In this paper, we use the B–splines transformation model [12] to locally register the globally aligned LV walls due to its flexibility and effectiveness for modeling large deformations. The basic idea of using B–splines is to deform an object by manipulating an underlying lattice, $\mathbf{\Phi}$, of control points, $\phi_{l,n}$: $l = 0, \ldots, L - 1$; $n = 0, \ldots, N - 1$, to maximize a new similarity function that accounts for 1st– and 2nd–order NMI. The B-splines deformation model is demonstrated as follows [12]:

$$f(x, y) = \sum_{i=-1}^{2} \sum_{j=-1}^{1} \beta_i(s)\beta_j(t)\phi_{l+i,n+j} \qquad (1)$$

where $l = \lfloor x \rfloor$, $n = \lfloor y \rfloor$, $\lfloor . \rfloor$ denotes the integer part of a real-valued number; (s, t): $s = x - l \in [0, 1)$ and $t = y - n \in [0, 1)$, is the relative position of the Cartesian point (x, y) with respect to the four nearest lattice points (l, n), $(l + 1, n)$, $(l, n + 1)$ and $(l + 1, n + 1)$;
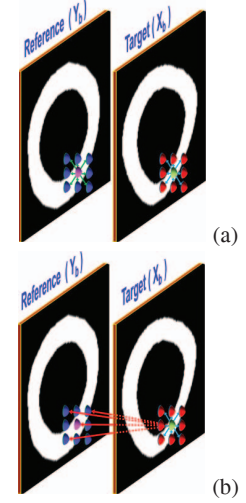
and $\beta_j(u)$ is the jth basis function; $u \in [0, 1)$; $j = -1, \ldots, 2$, of the uniform cubic B-spline [12]:

$$\beta_{-1}(u) = \tfrac{1}{6}(-u^3 + 3u^2 - 3u + 1); \quad \beta_0(u) = \tfrac{1}{6}(3u^3 - 6u^2 + 4);$$

$$\beta_1(u) = \tfrac{1}{6}(-3u^3 + 3u^2 + 3u + 1); \quad \beta_2(u) = \tfrac{1}{6}u^3$$

Similarity measure: We propose a new similarity metric (C) that accounts for both the 1st– and 2nd–order NMI between the reference ($\mathbf{Y}$) and the target ($\mathbf{X}$) images. Let $\mathbf{K} = \{0, 1\}$ and $\mathbf{R}$ denote finite sets of object ("1") and background ("0") labels, and a 2-D arithmetic lattice supporting an FP-MRI grayscale image and its goal binary "object-background" region map $\mathbf{m} : \mathbf{R} \rightarrow \mathbf{K}$, respectively. The proposed similarity metric is defined as follows:

$$C(\mathbf{Y}, \mathbf{X}) = \frac{H(\mathbf{Y}_g) + H(\mathbf{X}_g)}{H(\mathbf{Y}_g, \mathbf{X}_g)} + \frac{H(\mathbf{Y}_b) + H(\mathbf{X}_b)}{H(\mathbf{Y}_b, \mathbf{X}_b)} \qquad (2)$$

where $\mathbf{Y}_g$ and $\mathbf{X}_g$ are the reference and target gray scale images, respectively, and $\mathbf{Y}_b$ and $\mathbf{X}_b$ are the reference and target region map images, respectively. $H(.)$ is the Shannon entropy of the image signals, $H(.) = -\sum_{(x,y) \in \mathbf{R}} p_{x,y}(.) \log p_{x,y}(.)$, and $H(.,.)$ is their joint entropy, $H(.,.) = -\sum_{(x,y) \in \mathbf{R}} p_{x,y}(.,.) \log p_{x,y}(.,.)$.

Estimation of the 1st–order NMI: To accurately approximate the marginal, $p(\mathbf{Y}_g)$ and $p(\mathbf{X}_g)$, and joint, $p(\mathbf{Y}_g, \mathbf{X}_g)$, probability distributions of the gray levels, we use the linear combination of discrete Gaussians (LCDG) with positive and negative components. The parameters of the LCDG-models (mean and covariance) are estimated using a new version of the expectation maximization (EM) algorithm called the modified EM algorithm [13].

Estimation of the 2nd–order NMI: We use a generic Markov-Gibbs random field (MGRF) image model to accurately estimate the 2nd–order marginal, $p(\mathbf{Y}_b)$ and $p(\mathbf{X}_b)$, and joint, $p(\mathbf{Y}_b, \mathbf{X}_b)$, probability distributions (see Fig. 2). For simplicity and by symmetry considerations, the interaction structure is limited to the pixel's nearest 8–neighbors (Fig. 3(a)) for the estimation of $p(\mathbf{Y}_b)$ and $p(\mathbf{X}_b)$; while for the estimation of $p(\mathbf{Y}_b, \mathbf{X}_b)$ the structure includes 17–neighbors (8-neighbors in the target frame and 9- neighbors in the reference frame, Fig. 3 (b)). For both structures, Gibbs potentials are bi-valued and depend only on whether each pair of labels are equal or not. Under these assumptions, our model is similar to the Potts model and differs only in that the potentials are estimated analytically.
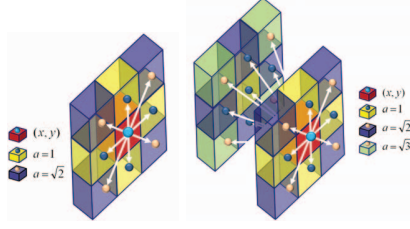
Fig. 3. Interaction neighborhood systems for the estimation of the MGRF marginal (left) and joint (right) probabilities.

The 8-neighborhood (Fig. 3(a)) has two types of symmetric pairwise interactions, specified by the absolute distance a between two pixels in a given map: (*i*) horizontal and vertical pairs with $a = 1$, and (*ii*) the diagonal pairs with $a = \sqrt{2}$. In addition to $a \in \mathbf{A} = \{1, \sqrt{2}\}$, the 17-neighborhood (Fig. 3(b)) has one more type of pairwise interactions between a given pixel location on the target map and the reference map with $a = \sqrt{3}$. Let $\mathbf{N} = \{\mathbf{N}_a, a \in A\}$ denote the family of the neighboring pixel pairs supporting the Gibbs potentials and $|\mathbf{C_N}|$ denote its cardinality. For simplicity, we will use $\mathbf{m}$ to refer to either $\mathbf{Y}_b$ or $\mathbf{X}_b$. The potentials of each type are bi-valued because only the coincidence of the labels is taken into account: $\mathbf{V}_a = \{V_{a,\text{eq}}; V_{a,\text{ne}}\}$ where $V_{a,\text{eq}} = V_a(k, k')$ if $k = k'$ and $V_{a,\text{ne}} = -V_a(k, k')$ if $k \neq k'$; $k \in \mathbf{K}$. Then, the marginal probability of the MGRF model of the region maps is as follows:

$$p(\mathbf{m}) = \frac{1}{Z} \exp \sum_{(x,y) \in \mathbf{R}} \sum_{(\xi,\eta) \in \mathbf{N}} V_a(m_{x,y}, m_{x+\xi,y+\eta}) \quad (3)$$

where Z is the approximate partition function [14]: $Z \approx e^{\left(V_a |\mathbf{C_N}| (2-K)\right)}$. The MGRF model is identified analytically by using the approximate maximum likelihood estimates of the potentials [14]: $V_{a,\text{eq}} = -V_{a,\text{ne}} = 2 \times f_{a,\text{eq}}(\mathbf{m}) - 1$; where $f_{a,\text{eq}}(\mathbf{m})$ denotes the relative frequency of the equal label pairs in the equivalent pixel pairs. Similarly the joint MGRF probability, $p(\mathbf{Y}_b, \mathbf{X}_b)$, can be estimated using Eq. (3) and the neighborhood system of Fig. 3 (b) with $a \in \mathbf{A} = \{1, \sqrt{2}, \sqrt{3}\}$. We used a gradient descent method to find the best resolution of the lattice $\mathbf{\Phi}$ (control points) to maximize the proposed similarity metric in Eq. (2). The B-splines based registration for the globally aligned frame shown in Fig. 6(c), using the proposed similarity metric, and the corresponding deformation field, are shown in Fig. 6(d) and (e), respectively.

2.2.2. Iso-contours based nonrigid registration

For accurate analysis of the perfusion data, we need to be sure that there is a one-on-one pixel match in all co-aligned LV walls. For this reason, we propose a new refinement registration step that will assure that there is a one-on-one pixel match between all registered frames of a given perfusion sequence. The refinement registration step is based on deforming each pixel of the target wall over evolving closed equi-spaced contours (iso-contours) to closely match the reference wall. To generate these closed iso-contours, the first step is to extract the centerline of both reference and target walls.

Centerline extraction: The main idea of the proposed centerline approach is to find point-to-point correspondences between the inner and outer borders of the LV wall. Then, the centerline is extracted by picking the points that are located equidistant from the two correspondence points (see e.g., Fig. 4 (c)). The point-to-point correspondences between the wall borders are estimated based on solving the 2nd-order Laplace equation: $\nabla^2 \gamma = \partial^2 \gamma / \partial x^2 + \partial^2 \gamma / \partial y^2 = 0$, for a scalar field γ. After the potential, $\gamma(x, y)$, between the borders is found by solving the Laplace equation, its gradient vectors induce the streamlines, linking the corresponding border points.

The process of the extraction of the centerline using the Laplace-based method is shown in Fig. 4. A distance map is generated inside the LV wall by finding for every inner point the minimum Euclidean distance to the wall boundaries (Fig. 4 (a)). The Laplace equation is then applied to wall borders to co-locate the corresponding border points (Fig. 4 (b)). Then, for each streamline linking corresponding border points, the streamline point located at equidistance from both borders is selected as a candidate location on the centerline (Fig. 4 (c)). Finally, the centerline is generated using a closed spline fit for the selected points, (Fig. 4 (d)).

Evolution of the generated iso-contours: Following the extraction of the centerline, a collection of equi–spaced contours (iso-contours) within the LV wall, generated at equal distances from the centerline, are formed (Fig. 5). Again, we use the Laplace equation applied to the corresponding iso-contours of the reference and target LV walls to co-locate the corresponding contour points. The result of the proposed iso-contours based nonrigid registration is shown in Fig. 6 (f).

3. EXPERIMENTAL RESULTS AND CONCLUSIONS

The proposed framework was tested on cross-sectional FP-MRI data, with a typical 60 time frames, obtained from patients with prior myocardial infarctions, documented by viability MRI, who were undergoing a novel myoregeneration therapy. Short-axis images were obtained using a 1.5T Espree system, Siemens Medical Solutions, USA Inc., with phased array wrap-around reception coils: slice thickness 10 mm, in-plane resolution 1.87×1.87 mm^2, FOV 308×379 mm^2, and image size of 512×512 pixels.
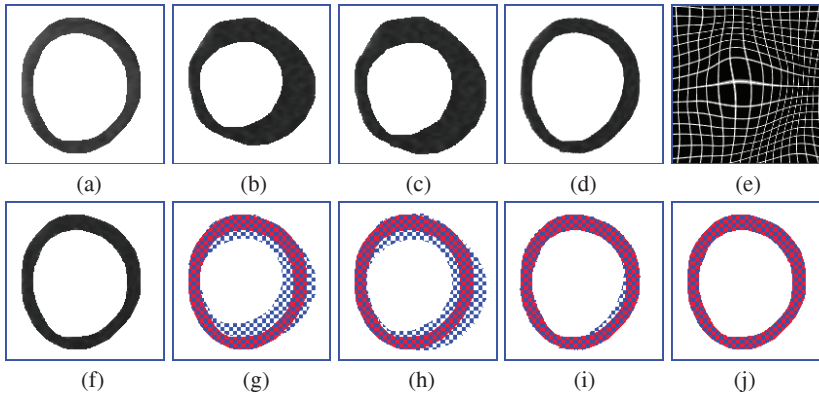
Basic steps of the proposed registration sequence for one of the 60 image frames are demonstrated in Fig. 6. To highlight the advantages of our approach, checkerboard displays before and after each step of the proposed registration are shown in Fig. 6(g) through (j). The reference object is shown in red and the target object is shown in blue. Figure 6(g) shows the superimposed target and reference walls before any registration steps are applied. Figure 6(h) shows the effect of the global alignment with some resultant improvement of matching the edges. Figure 6(i) shows further marked improvement after the B-splines registration step. Figure 6(j), with a further application of the Laplace–based local alignment of contours, shows a near ideal match of the target and reference contours.

Since the ultimate goal of the proposed framework is to improve the visualization of transmural perfusion gradients on FP-MRI, the co-aligned frames can allow us to construct signal intensity versus time plots (see Fig. 1) and to derive perfusion-related indexes (e.g., initial up-slope, peak signal intensity, and time-to-peak signal, and the average plateau signal intensity change, see Fig. 1) from these perfusion curves. For visual assessment of the perfusion-related indexes, we use pixel-wise parametric maps that represent the regional wall transit of the contrast agent. An example of the pixel-wise parametric images for the peak signal intensity for one of the test datasets before and after applying the proposed registration approach is shown in Fig. 7. The figure clearly demonstrates a more continuous and homogenous appearance of the perfusion index map after registration when compared with that before registration.

In total, we propose a novel framework for the accurate non-rigid registration of cardiac first-pass perfusion MRI for improved visualization of perfusion gradients of these time series images. The proposed framework employs an initial 2D affine, rigid registration to account for the global motion of the heart, and a local nonrigid registration to handle the local deformations of the LV wall using a B-spline transformation model that maximize a new similarity metric. The latter accounts for the 1st and 2nd order NMI between the globally registered frames. This is followed by a refinement step that
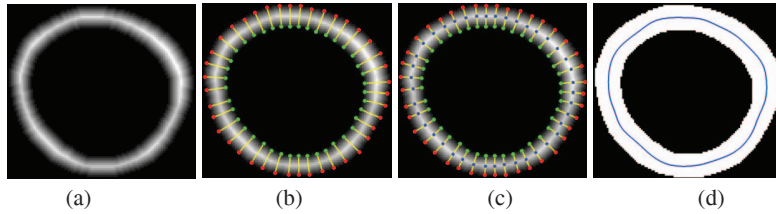
Fig. 4. Illustration of the centerline extraction: (a) distance map of a typical LV wall, (b) streamlines found by solving Laplace equation, (c) the identified centerline points (blue), and (d) the extracted centerline.
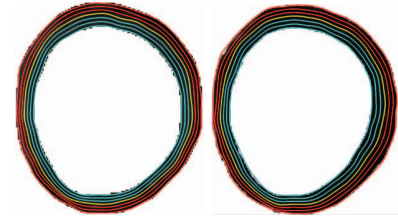

Fig. 5. An example of the generated iso-contours for the reference (left) and target (right) LV walls. The centerline is shown in yellow.

Fig. 6. Step-by-step registration for one target image to the reference: (a) reference image, (b) target image, (c) global registration applied to the target, (d) B–splines registration, (e) obtained deformation field used for the B-splines registration, and (f) Laplace-based registration. Subsequent checkerboard visualization of the superimposed target and reference walls before global (g), after global (h), after B–splines (i) and after iso-contours (j) registration.

Fig. 7. Parametric maps for the peak signal intensity index obtained before (a) and after (b) the proposed registration for one test dataset. The red and blue colors of the color scale reflect high and low values, respectively.

is based on deforming the target wall over evolving iso-contours, using a Laplace method, to more closely match the reference wall.
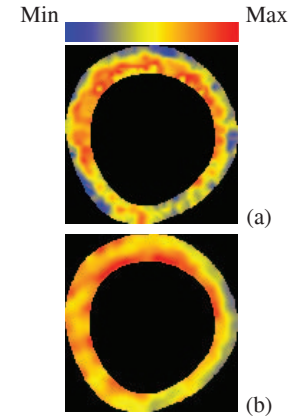
Our future work will explore the effectiveness of the proposed approach for analyzing perfusion-related indexes of both the transient phase– peak signal intensity, time-to-peak, and initial up-slope– and the more slowly varying phase (plateau phase), as indexed using the signal change during this phase. Also, we will study the usefulness of pixel-by-pixel image displays of the derived perfusion indexes to investigate both regional perfusion differences and transmural manifestation, and improvement with treatment.

4. REFERENCES

[1] M. Breeuwer, L. Spreeuwers, and M. Quist, "Automatic quantitative analysis of cardiac MR perfusion images", *Proc. SPIE Med. Imag.*, pp. 733–742, 2001.

[2] K. K. Wong, E. S. Yang, E. X. Wu, H.-F. Tse, and S. T. Wong, "First-pass myocardial perfusion image registration by maximization of normalized mutual information", *J. Magn. Reson. Imag.*, vol. 27, pp. 529–537, 2008.

[3] L. M. Bidaut and J. P. Valle, "Automated registration of dynamic MR images for the quantification of myocardial perfusion", *J. Magn. Reson. Imag.*, vol. 13, pp. 648–655, 2001.

[4] C. M. Gallippi, C. M. Kramer, Y. L. Hu, D. A. Vido, N. Reichek, and W. J. Rogers, "Fully automated registration and warping of contrast-enhanced first–pass perfusion images", *J. Cardiovasc. Magn. Reson.*, vol. 4, pp. 394–410, 2002.

[5] M. Stegmann, H. Ólafsdóttir, and H. Larsson, "Unsupervised motion-compensation of multi-slice cardiac perfusion MRI", *Med. Image Anal.*, vol. 9, pp. 459–569, 2005.

[6] G. Adluru, E. V. DiBella, and M. C. Schabel, "Model-based registration for dynamic cardiac perfusion MRI", *J. Magn. Reson. Imag.*, vol. 24, pp. 1062–1070, 2006.

[7] J. Milles, R. J. van der Geest, M. Jerosch-Herold, J. H. Reiber, and B. F. Lelieveldt, "Fully automated motion correction in first-pass myocardial perfusion MR image sequences", *IEEE Trans. Med. Imag.*, vol. 27, pp. 1611–1621, 2008.

[8] G. Wollny, M. J. Ledesma-Carbayo, P. Kellman, and A. Santos, "Exploiting quasiperiodicity in motion correction of free-breathing myocardial perfusion MRI", *IEEE Trans. Med. Imag.*, vol. 29, pp. 1516–1527, 2010.

[9] G. Tarroni, A. R. Patel, F. Veronesi, J. Walter, C. Lamberti, R. M. Lang, V. Mor-Avi, and C. Corsi, "MRI-based quantification of myocardial perfusion at rest and stress using automated frame-by-frame segmentation and non-rigid registration", *Comput. in Cardiol.*, vol. 37, pp. 1–4, 2010.

[10] F. Khalifa, G. M. Beache, G. Gimel'farb, K. Welch, and A. El-Baz "Automatic segmentation of the heart wall from cardiac first-pass perfusion MRI," *under review ICIP'12*.

[11] C. Studholme, D. L. G. Hill and D. J. Hawkes, "An overlap invariant entropy measure of 3-D medical image alignment", *Pattern Recogn.*, vol. 32, pp. 71–86, 1999.

[12] S. Lee, G. Wolberg, K.-Y. Chwa, and S. Y. Shin , "Image metamorphosis with scattered feature constraints," *IEEE Trans. Vis. Comput. Graph.,* vol. 2, pp. 337-354, 1996.

[13] A. El-Baz and G. Gimel'farb, "EM based approximation of empirical distributions with linear combinations of discrete Gaussians", *Int. Conf. Image Process.*, pp. 373–376, 2007.

[14] A. Farag, A. El-Baz, and G. Gimel'farb, "Precise segmentation of multimodal images," *IEEE Trans. Image Process.,* vol. 15, pp. 952-968, 2006.